

# StainNet: a fast and robust stain normalization network

HONGTAO KANG,<sup>1,2</sup> DIE LUO,<sup>1,2</sup> WEIHUA FENG,<sup>1,2</sup> JUNBO HU,<sup>3,\*</sup> SHAOQUN ZENG,<sup>1,2</sup> TINGWEI QUAN,<sup>1,2</sup> AND XIULI LIU<sup>1,2,\*</sup>

<sup>1</sup>*Britton Chance Center for Biomedical Photonics, Wuhan National Laboratory for Optoelectronics-Huazhong University of Science and Technology, Wuhan, Hubei 430074, China*

<sup>2</sup>*MOE Key Laboratory for Biomedical Photonics, Collaborative Innovation Center for Biomedical Engineering, School of Engineering Sciences, Huazhong University of Science and Technology, Wuhan, Hubei 430074, China*

<sup>3</sup>*Department of Pathology, Hubei Maternal and Child Health Hospital, Wuhan, Hubei 430072, China*

*\*Corresponding authors: Junbo Hu(cqjbhu@163.com), Xiuli Liu(xliu@mail.hust.edu.cn)*

**Abstract:** Due to a variety of factors, pathological images have large color variabilities, which hamper the performance of computer-aided diagnosis (CAD) systems. Stain normalization has been used to reduce the color variability and increase the accuracy of CAD systems. Among them, the conventional methods perform stain normalization on a pixel-by-pixel basis, but estimate stain parameters just relying on one single reference image and thus would incur some inaccurate normalization results. As for the current deep learning-based methods, it can automatically extract the color distribution and need not pick a representative reference image. While the deep learning-based methods have a complex structure with millions of parameters, and a relatively low computational efficiency and a risk to introduce artifacts. In this paper, a fast and robust stain normalization network with only 1.28K parameters named StainNet is proposed. StainNet can learn the color mapping relationship from a whole dataset and adjust the color value in a pixel-to-pixel manner. The proposed method performs well in stain normalization and achieves a better accuracy and image quality. Application results show the cervical cytology classification achieved a higher accuracy when after stain normalization of StainNet.

© 2020 Optical Society of America under the terms of the [OSA Open Access Publishing Agreement](#)

## 1. Introduction

Tissues or cells are often transparent and must be stained before they can be observed under a microscope. However, inconsistencies in the stain reagents, staining process, and scanner specifications often result in different appearances of pathological images [1]. These variations affect the judgment of pathologists, weak the performance of CAD systems, and hamper their applications in pathology [2-4]. Currently, stain normalization algorithms have been proposed to reduce color variation in pathological images. Usually, they transfer the color style of the source image to that of a target image [5] while preserve the other information in the processed image [6]. It is reported that stain normalization helps to increase the prediction accuracy, such as tumor classification, so it has been an important preprocessing task, especially for CAD systems [7]. Stain normalization methods can be broadly classified into two classes: conventional methods and deep learning-based methods.

Conventional methods include Color matching and Stain-separation methods. Color matching methods try to match the color distribution of the source image to that of a reference image [8]. For example, Reinhard et al. [9] calculated the mean and standard deviations of source images and matched them to a reference image in the Lab color space. Stain-separation methods try to separate and normalize each staining channel independently. For instance, Ruifrok and Johnston [10] proposed to measure the relative proportion for three channels (R, G, and B) with the slides stained by only single stain reagent (Hematoxylin or Eosin only) to

estimate stain vectors. On the other hand, Macenko et al. [11], Vahadane et al. [12], and Khan et al. [5] used mathematical methods to compute stain vectors. Macenko et al. [11] found the stain vectors by singular value decomposition (SVD) in Optical Density (OD) space. And Vahadane et al. [12] applied sparse non-negative matrix factorization (SNMF) to compute the stain vectors. Khan et al. [5] used a pertained classifier to estimate the relative intensity of the two stains (Hematoxylin and Eosin) to obtain an estimate of the stain vectors. However, Pap stain used in cervical cytopathology involves not only Hematoxylin and Eosin but also Orange, Light Green, and Bismarck Brown [13], which is the main reason why conventional algorithms do not perform well on cervical cytopathology. Nevertheless, most of these rely on a reference image to estimate stain parameters, but it's hard for one reference image to cover all staining phenomena or represent all input images, which usually causes misestimation of stain parameters and thus delivers inaccurate normalization results [14,15].

Deep learning-based methods mostly use generative adversarial networks (GAN) to achieve stain normalization [3,6,8,16-18]. Shaban et al. [8] proposed an unsupervised stain normalization method named StainGAN based on CycleGAN [16]. Furthermore, Cai et al. [3] proposed a new generator, which obtained a better image quality and accelerated the networks. On the other hand, Shaojin et al. [18], Salehi et al. [6] and Tellez et al. [17] reconstructed original images from the images with color augmentations applied, e.g. grayscale and Hue-Saturation-Value (HSV) transformation, and tried to normalize all other color styles to original. However, due to the complexity of deep neural networks and the instability of GANs, it is hard to preserve the source information, and it has a risk to introduce some artifacts, which have some adverse effects for pathological diagnosis [19]. Nevertheless, the network of deep learning-based methods usually contains millions of parameters, so it has low efficiency in computation [14].

Deep learning-based methods perform well in stain normalization, but they are not satisfactory in the robustness and computational efficiency. Considering this, in this paper, we propose a novel stain normalization network named StainNet. The computational efficiency was improved by using a fully  $1 \times 1$  convolutional network, which achieved stain normalization in a pixel-to-pixel manner. Further, by learning the normalized images of deep learning-based methods, the color mapping relationship was acquired precisely. The experimental results on cervical cytology images showed that StainNet better preserved the source information and was more similar to target images. Computation results demonstrated StainNet was more than 40 times faster than StainGAN [8]. And then after the color normalization of StainNet, the cervical cytology classification achieved a higher accuracy.

## 2. Approach

Usually, the current deep learning-based methods apply a convolution with kernel size  $3 \times 3$  or larger. The  $3 \times 3$  convolution performs weighted summation on the local  $3 \times 3$  neighborhood of the input image. So, it's inevitably that values are affected by the local texture. Unlike  $3 \times 3$  convolution,  $1 \times 1$  convolution only maps a single pixel and has nothing to do with the local neighborhood values. That is, it will not be affected by the texture. In this paper, stain normalization is regarded as a color space transformation, which usually refers to the transformation from one color space to another using linear or nonlinear transformations [20]. It is better just only to transfer the color value and not change the texture or content around the pixel in the source image. Following this idea, we propose a stain normalization network named StainNet which uses  $1 \times 1$  convolution to transform the source color space into several intermediate color spaces, then from the intermediate color space to the target color space. In this paper we use two intermediate color spaces with 32 channels by default.

StainNet needs paired source and target images to learn the transformation from the source color space to the target color space. It's hard to get the paired images and hard to align the images perfectly. For learning the color mapping relationship, we propose an unsupervised method to train StainNet, as shown in Fig.1. The training process mainly consists of three steps.

Firstly, we trained a generator with unpaired source and target images using StainGAN [8]. Then, the generator was used to normalize the source images. At last, the normalized images were taken as the Ground Truths to train StainNet with L1 Loss and SGD optimizer.

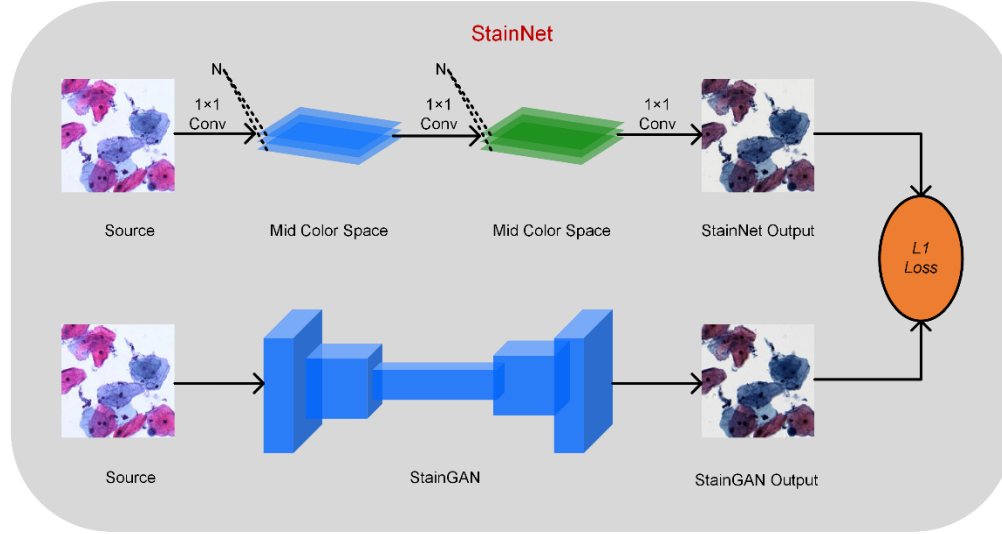


Fig. 1. The network structure and training process of StainNet

### 3. Experiments and Results

In this section, StainNet was compared with the state-of-the-art methods of StainGAN [8], Reinhard [9], Macenko [11], and Vahadane [12].

#### 3.1 Evaluation Metrics

In order to evaluate the performance of different methods, we measured the similarity between the normalized image and the target image, and the consistency between the normalized image and the source image.

Specifically, two similarity metrics were used: Structural Similarity index (SSIM) [21], Peak Signal-to-Noise Ratio (PSNR). The SSIM and PSNR of the target image (SSIM Target and PSNR Target) were used to evaluate the similarity between the normalized image and the target image. The extent of source information preservation is weighed by the SSIM of the source image (SSIM Source), which also was used to measure the similarity between the normalized image and the source image. Unlike calculating SSIM Target and PSNR Target by using the original RGB values, the normalized image and the source image were transformed into grayscale and linearly mapped the pixel values of each image into 0~255 when calculating SSIM Source.

#### 3.2 Datasets

Two slide scanners were used to scan the cervical cytopathology slides from Maternal and Child Hospital of Hubei Province. One scanner was custom-constructed by our group, called Scanner O, used a 20x objective lens with a resolution of 0.2930  $\mu\text{m}$  per pixel. The other was from TEKSQRAY Ltd, called scanner T, used a 40x objective lens with a resolution of 0.1803  $\mu\text{m}$  per pixel. The images from scanner T were resized to the resolution of 0.2930  $\mu\text{m}$  per pixel, then rigid and no-rigid registration were performed to align the images from scanner T to these from scanner O. Finally, 3223 precisely registered image pairs with dimensions of 512 $\times$ 512 were collected. Among the images, 2257 pairs were randomly extracted as the training dataset and 966 image pairs were used as the test dataset. To map the patches from scanner O to these

from Scanner T, the patches from scanner O are used as source images and these from scanner T are used as target images.

### 3.3 Implementation

For conventional methods Reinhard [9], Macenko [11], and Vahadane [12], the target image was used as a reference image. StainGAN [8] was trained with the same parameters as [8].

For our method, we first used the trained StainGAN to normalize the source images in both the training dataset and the test dataset. Then we used the normalized images as the Ground Truths during training. StainNet was trained with stochastic gradient descent (SGD) optimizer, an initial learning rate of 0.01, and a batch size of 10. L1 loss was used to minimize the difference between the output of network and the normalized image by StainGAN. Cosine annealing scheduler was adopted to decay learning rate from 0.01 to 0 during 300 epochs. The PSNR was calculated to evaluate the output of StainNet against the normalized image by StainGAN in the test dataset and the checkpoint with best PSNR was chosen experimentally.

Frames per second (FPS) was calculated on the system with 6-core Intel(R) Core (TM) i7-6850K CPU and NVidia GeForce GTX 1080Ti. Input and output (IO) time was not included.

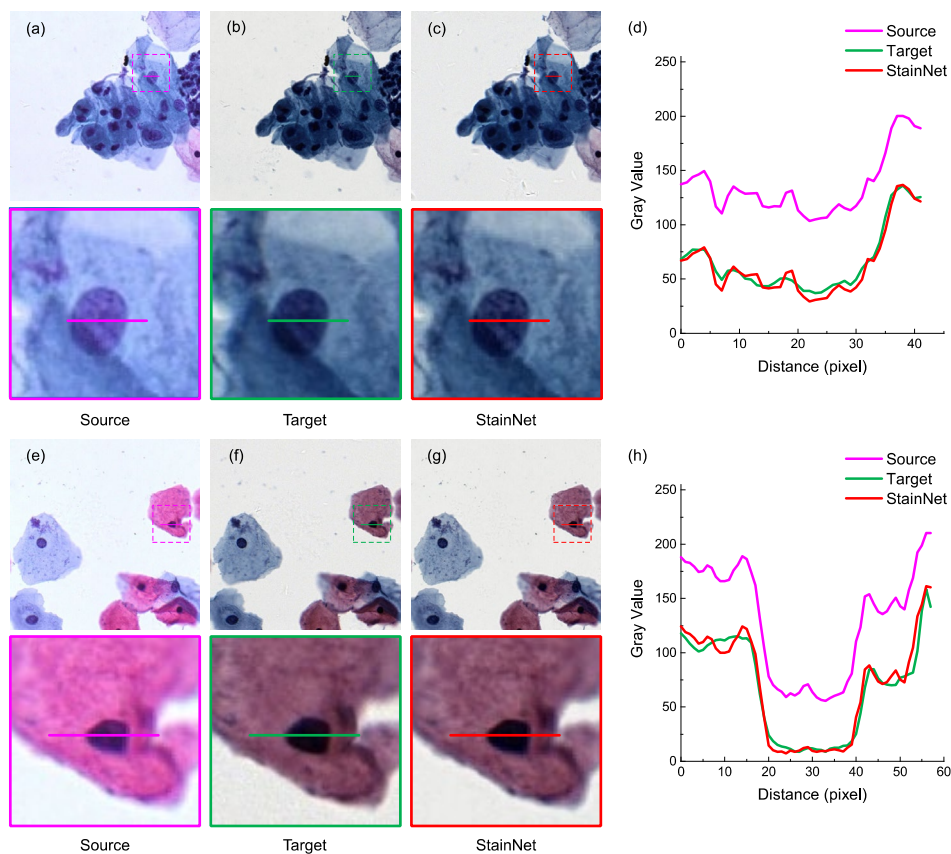


**Fig. 2.** StainNet stain normalization effect on cervical cells. The source images, the target images, and the normalized images by StainNet are shown in (a, e), (b, f), and (c, g), respectively. The image in the dashed box is enlarged below. Gray value profiles of the straight lines on (a-c) are shown in the line chart (d) and the straight lines in (e-g) are shown in the line chart (h).

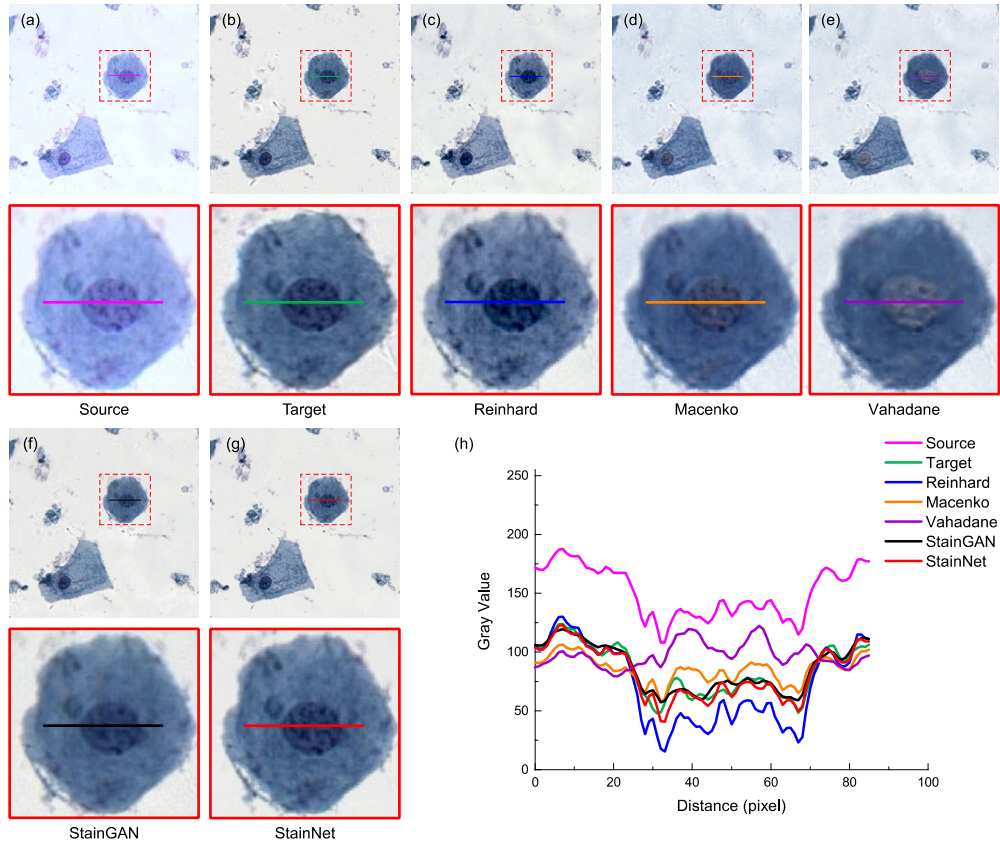


**Fig. 3.** Visual comparison of different normalization methods. Source image (a), target image (b), and normalized image by Reinhard (c), Macenko (d), Vahadane (e), StainGAN (f) and StainNet (g) are listed. The conventional methods Reinhard, Macenko, and Vahadane use the target image (b) as the reference image. The images below are enlargement of the red dashed box. Gray value profiles of the straight lines in (a-g) are shown in the line chart (h).

**Table 1.** Different evaluation metrics are reported for various stain normalization methods

Methods	SSIM Target	PSNR Target	SSIM Source	FPS
Reinhard	0.779	27.6	0.955	54.8
Macenko	0.771	25.9	0.919	4.0
Vahadane	0.776	26.0	0.927	0.5
StainGAN	0.758	29.4	0.913	19.6
<b>StainNet</b>	<b>0.808</b>	<b>29.8</b>	<b>0.960</b>	<b>881.8</b>

### 3.4 Results

StainNet stain normalization results are shown in Fig. 2. Visual comparison of source images, target images, and the normalized images shows StainNet obtain visually similar images to the target images. And the gray value profiles in Fig. 2 (d, h) show that StainNet can keep all most texture of the source images.

Further, StainNet was compared with the other normalization methods, illustrated in Fig. 3. Normalized images and their gray value profiles show that our results outperform the other methods on both the similarity to the target image and the preservation of the source information. For quantitative evaluation, the similarity metrics and frames per second (FPS) are reported in Table 1, where StainNet got all the highest metrics. It means that our method can preserve most information of the source image while being similar to the target image. Besides that, our method is 40 times faster than StainGAN in processing speed which is important for real-time stain normalization.

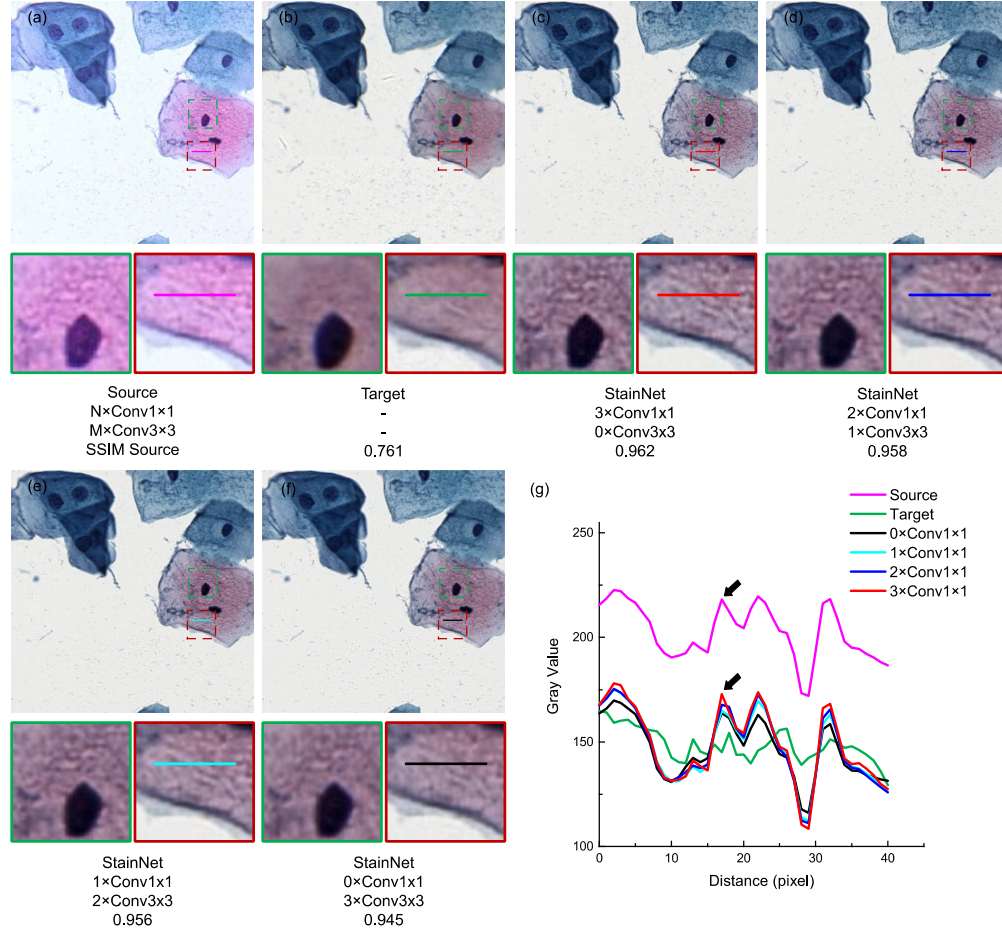


**Fig. 4.** Effects of  $1\times 1$  and  $3\times 3$  convolutions.  $N\times\text{Conv}1\times 1$  and  $M\times\text{Conv}3\times 3$  refers to the number of  $1\times 1$  convolution and  $3\times 3$  convolution. StainNet contains only three convolution layers, so the total number of  $1\times 1$  convolution and  $3\times 3$  convolution is three, that is,  $M+N=3$ . The image in the dashed box is enlarged below. Gray value profiles of the straight lines in (a-f) are shown in the line chart (g).

### 3.5 Structure Discussion

In this section, we conduct a comparative experiment to verify the role of  $1\times 1$  convolution in stain normalization. The effectiveness of  $1\times 1$  convolution is verified by replacing the three  $1\times 1$  convolution in StainNet with  $3\times 3$  convolutions in turn. The source image, target image, and normalized image by different structure of StainNet are shown in Fig. 4 (a-f), and the gray value profiles of the straight lines in Fig. 4 (a-f) are shown in Fig. 4 (g). It is clearly that with the increase of  $3\times 3$  convolution, the normalized image becomes more blurred, and the ability to

preserve the source information is getting worse. The best image quality can be obtained fully using  $1 \times 1$  convolution in Fig. 4 (c). In particular, at the place pointed by the black arrow in Fig. 4 (g), only a fully  $1 \times 1$  convolutional network can best preserve the grayscale changes of the source image. The different evaluation metrics, SSIM Target, PSNR Target, and SSIM Source, for different structure of StainNet are reported in Table 2. Although the  $3 \times 3$  convolutions may help improve the similarity with the target images, it affects the ability to preserve the source information. Not changing the information of the source image is a basic requirement for stain normalization, so a fully  $1 \times 1$  convolutional network is chosen.

**Table 2. Evaluation metrics of different StainNet structures.**

Number of Conv $1 \times 1$	Number of Conv $3 \times 3$	SSIM Target	PSNR Target	SSIM Source
3	0	0.808	29.8	0.960
2	1	0.814	30.0	0.958
1	2	0.814	30.0	0.956
0	3	0.804	29.8	0.950

## 4. Application

Can stain normalization further improve the performance of CAD system after reducing the color variation of pathological sections in different hospitals and different scanners? In this section, our method is compared with StainGAN on the task of cervical cytology classification.

### 4.1 Dataset

We used the same scanner specifications as in Section 3.2, and the patches from scanner T were used as the training dataset and these of scanner O as the test dataset. There are 6589 abnormal patches and 6589 normal patches in the training dataset and 3343 abnormal patches and 3192 normal patches in the test dataset. The resolution of patches was resized to 0.4862  $\mu\text{m}$  per pixel with dimensions of  $256 \times 256$ . In this dataset, our goal is to classify the patches into abnormal and normal patches.

### 4.2 Experiments

For a classifier on this dataset, there are two approaches to enhance its robustness to color variations. One is to transfer the other style images to the same one via stain normalization, and the other is to train a classifier by color augmentations.

In order to verify the effect of stain normalization and color augmentations to a classifier, recently, Tellez et al. [17] and Gupta et al. [22] have comprehensive comparison of the effects of stain normalization and color augmentations. Following it, we have used two sets of augmentations:

1. Brightness-Rotation (BR): Brightness and contrast in the range [0.75, 1.25], and random rotations in the range [-180, 180] are applied together in this set of augmentation.
2. Brightness-Rotation-HED (BRH): Besides BR augmentation, the three components, hematoxylin, eosin, and dab in HED space [23] are also applied uniformly in the range [0.75, 1.25]. The sample images applied to these augmentations are shown in Fig. 5.

We carried out three experiments to analyze the impact of stain normalization and color augmentations, listed as below:

1.  $E_1$  The original (un-normalized) images in the training dataset are used to train the classifier.

2.  $E_2$  The original (un-normalized) images applied BR augmentation with a probability of 0.25 in the training dataset are used to train the classifier.
3.  $E_3$  The original (un-normalized) images applied BRH augmentation with a probability of 0.25 in the training dataset are used to train the classifier.

The original (un-normalized) and normalized images by StainGAN and StainNet in the test dataset are used to evaluate the classifier. And the StainGAN and StainNet trained in Section 3.3 were used to normalize the images on the test dataset. The sample original and normalized images by StainGAN and StainNet are shown in Fig. 6. From the figure, we can see that the normalized images by StainGAN and StainNet are close to the original images in the training dataset.

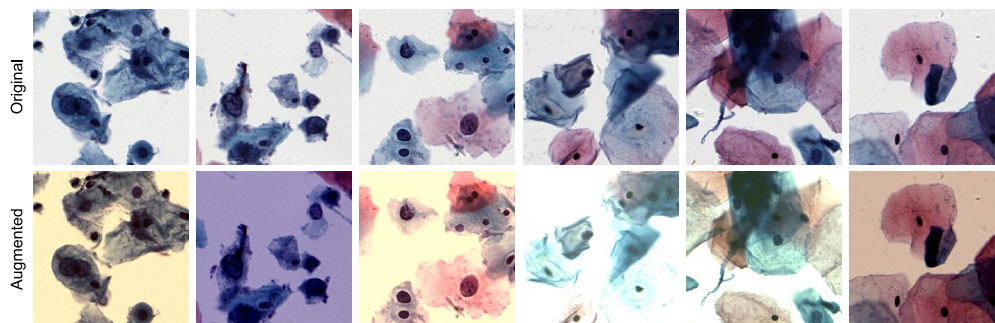


**Fig. 5.** The original and augmented images in the training dataset. The original images and the corresponding augmented images are shown in the first and second rows. The first three columns are abnormal patches, and the last three columns are normal patches. The random rotations are not applied for visualization purpose.

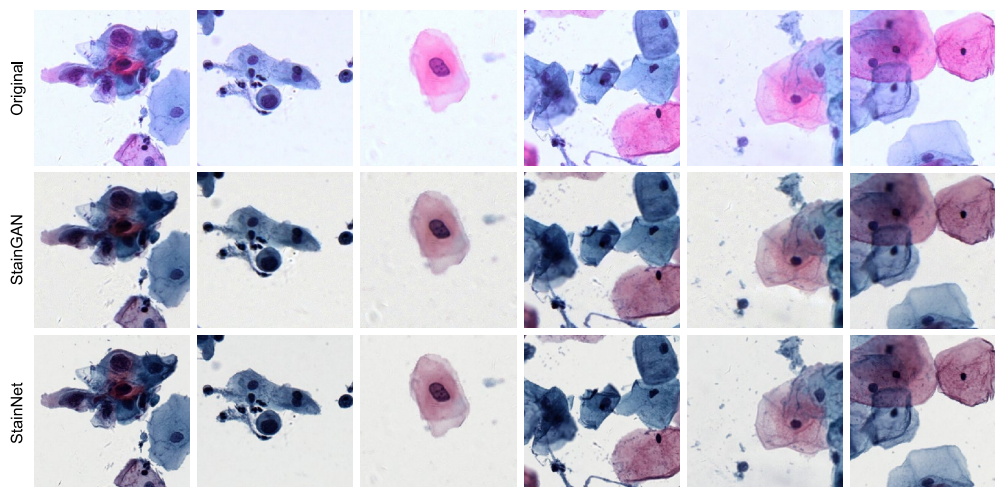


**Fig. 6.** The original and normalized images in the test dataset. The original images are shown in the first row, the normalized images by StainGAN are shown in the second row, and the normalized images by StainNet are shown in the third row. The first three columns are abnormal patches, and the last three columns are normal patches.

We used a pretrained ResNet50 [24] on ImageNet [25] as the classifier and fine-tuned it on the images in the training dataset. The classifier was trained with Adam optimizer, an initial learning rate of  $2e-4$  and a batch size of 64. Cross-entropy loss was used as our loss function. The learning rate was decreased by a factor of 0.1 at the 40th and the 50th epoch. The training was stopped at the 60th epoch, and we saved the checkpoint with the highest F1 score on the test dataset during the training.

### 4.3 Results

The classifier performance on the original and normalized test dataset by StainGAN and StainNet is quantitative evaluated in Table 3. In the table, we used recall, precision, accuracy, and F1 score as the performance metrics. It proves that color augmentations improve the classifier performance on the original test dataset, and stain normalization further improve the classifier performance. For the original test dataset, the accuracy was improved from 82.4% with the original training dataset ( $E_1$ ) to 88.8% with the BR augmented training dataset ( $E_2$ ) and 91.2% with the BRH augmented training dataset ( $E_3$ ). For the normalized test dataset, a better accuracy always could be obtained among all three experiments. Especially in experiment  $E_3$ , the highest accuracy and F1 score was obtained with StainNet normalization and BRH color augmentations, which was 93.1%. In original training dataset ( $E_1$ ), the test dataset normalized by StainGAN had a better accuracy and F1 score. That's probably because StainGAN is more similar to the training images in terms of texture. In the BR and BRH augmented training dataset ( $E_1, E_2$ ), StainNet performs better on the test normalized dataset. Besides that, in Table 3, StainNet obtained all the highest metrics and marked in bold case numbers.

**Table 3. Performance of the classifier trained in experiments  $E_1$  to  $E_3$ , with the original, color augmented training dataset. The images in the original and normalized test dataset by StainGAN and StainNet are used to test the classifier. The highest metric values obtained on the test dataset among all three experiments are marked in bold case numbers.**

$E_1$ Trained on the original training dataset				
Test dataset	Recall	Precision	Accuracy	F1 score
Original	0.767	0.874	0.824	0.817
StainGAN	0.919	0.910	0.912	0.914
StainNet	0.773	<b>0.923</b>	0.851	0.841
$E_2$ Trained on the BR augmented training dataset				
Test dataset	Recall	Precision	Accuracy	F1 score
Original	0.859	0.918	0.888	0.887
StainGAN	0.957	0.893	0.919	0.923
StainNet	0.955	0.902	0.924	0.928
$E_3$ Trained on the BRH augmented training dataset				
Test dataset	Recall	Precision	Accuracy	F1 score
Original	0.911	0.917	0.912	0.914
StainGAN	0.958	0.900	0.924	0.928
StainNet	<b>0.961</b>	0.909	<b>0.931</b>	<b>0.934</b>

## 5. Discussion and Conclusion

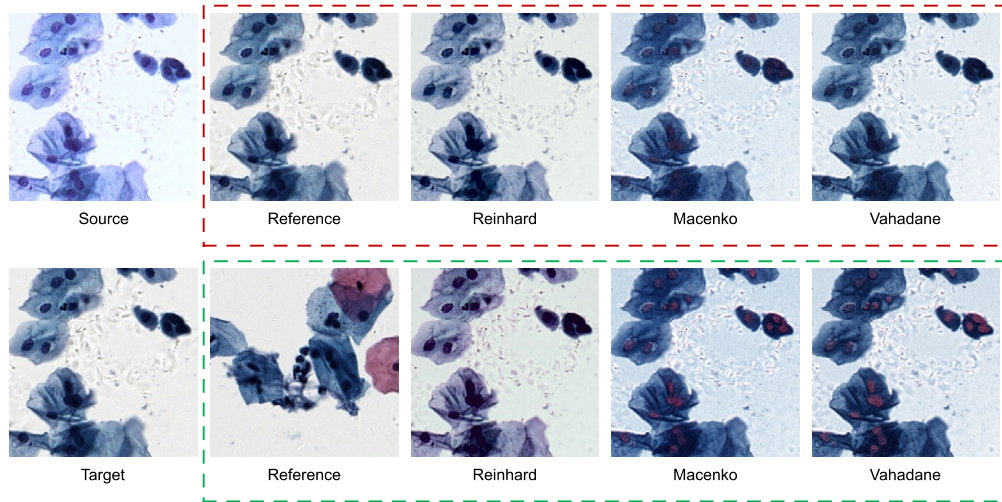


**Fig. 7.** The effect of the reference image on conventional methods. In the red dashed box, the target image is used as a reference image. In the green dashed box, an image close to the target image is used as a reference image.

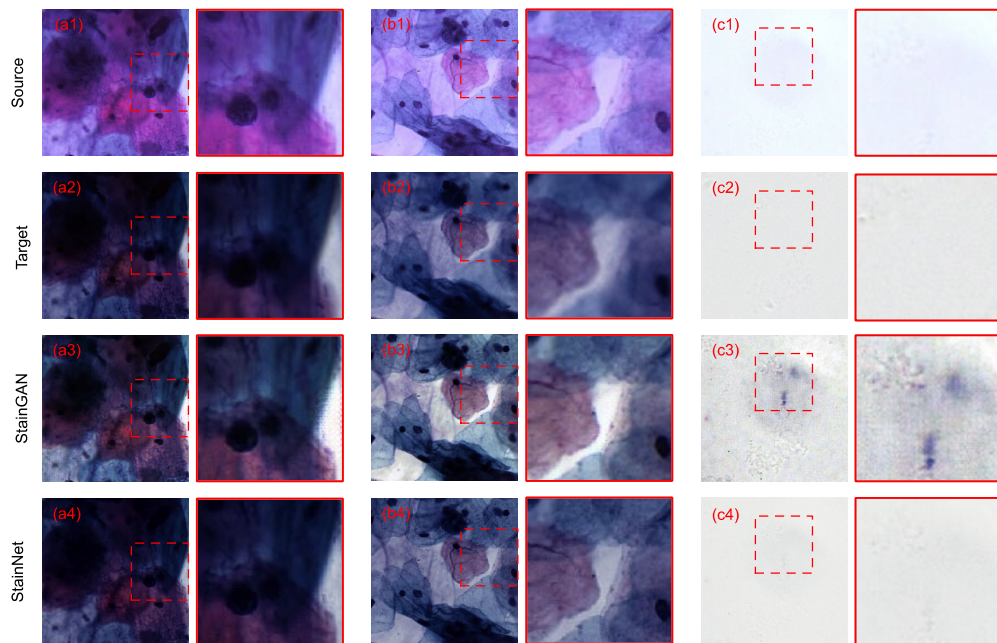


**Fig. 8.** The sample images normalized by StainGAN and StainNet. The image in the red dashed box is enlarged on the right. The source images, the target images, the normalized images by StainGAN, the normalized images by StainNet are shown in (a1, b1, c1), (a2, b2, c2), (a3, b3, c3), and (a4, b4, c4), respectively. The images normalized by StainGAN have artifacts in (a3), abnormal brightness in (b3), and noise in (c3). The images normalized by StainNet (a4, b4, c4) are more similar to the target images (a2, b2, c2).

Conventional methods rely on a reference image to estimate stain parameters, so the reference image has a huge impact on normalization results. The images in Section 3.2 are used to analyze effects of reference images on the normalized results, and the effect of using and not using the target image as the reference image on the normalization results is shown in Fig. 7. When using the reference image in the red dashed box, the stain normalization result is severely degraded.

The blue nucleus in the source image was turned into deep red nucleus just because of the two red cells in the reference image.

Further, the robustness of StainNet and StainGAN was compared using the test dataset mentioned in Section 4.1. The images normalized by StainGAN and StainNet are shown in Fig. 8. From the figure, we can see some normalized images by StainGAN have artifacts, abnormal brightness and noise, but the normalized image by StainNet is highly similar to the target image. Maybe it is because StainNet use a fully  $1 \times 1$  convolutional network, and thus not be affected by the texture or content of the input image. StainGAN would obtain wrong mapping due to the complexity of deep neural networks and the instability of GANs especially in the background and some borders.

In this paper, we achieve stain normalization by using a fully  $1 \times 1$  convolutional network in a pixel-to-pixel manner, which not only avoids the low computational efficiency and possible artifacts of deep learning-based methods, but also preserves well the information of the source image. Compared with conventional methods, StainNet learns the mapping relationship from the whole dataset instead of relying on one single reference image, so it can obtain the normalized image with high similarity. Furthermore, StainNet has been validated on the task of cervical cytology classification, and the results show that both stain normalization and color augmentations can significantly improve the performance of the classifier for color variations. Especially, the classifier trained on the BRH augmented training dataset got the highest accuracy on the test dataset normalized by StainNet. Since our method learns the mapping relationship between two color styles, it can only be applied to transfer from one color style to another. Therefore, in the scene when multiple color styles need to be normalized to one, it is necessary to train multiple networks to convert each color style individually.

## Funding

National Natural Science Foundation of China (NSFC) (61721092); Director Fund of Wuhan National Laboratory for Optoelectronics; Research Fund of Huazhong University of Science and Technology.

## Disclosures

The authors declare that there are no conflicts of interest related to this article.

## Data Availability

The source code of the StainNet network employed in this paper is available at Github: <https://github.com/khtao/StainNet>.

## References

1. M. Salvi, N. Michielli, and F. Molinari, "Stain Color Adaptive Normalization (SCAN) algorithm: Separation and standardization of histological stains in digital pathology," *Comput. Methods Programs Biomed.* 193, 105506 (2020).
2. F. Ciompi, O. Geessink, B. E. Bejnordi, G. S. De Souza, A. Baidoshvili, G. Litjens, B. Van Ginneken, I. Nagtegaal, and J. Van Der Laak, "The importance of stain normalization in colorectal tissue classification with convolutional networks," in *Proceedings - International Symposium on Biomedical Imaging (2017)*, pp. 160–163.
3. S. Cai, Y. Xue, Q. Gao, M. Du, G. Chen, H. Zhang, and T. Tong, "Stain Style Transfer Using Transitive Adversarial Networks," in *Machine Learning for Medical Image Reconstruction*, F. Knoll, A. Maier, D. Rueckert, and J. C. Ye, eds. (Springer International Publishing, 2019), pp. 163–172.
4. S. M. Ismail, A. B. Colclough, J. S. Dinnen, D. Eakins, D. M. Evans, E. Gradwell, J. P. O'Sullivan, J. M. Summerell, and R. G. Newcombe, "Observer variation in histopathological diagnosis and grading of cervical intraepithelial neoplasia," *BMJ* 298 (6675), 707–710 (1989).
5. A. M. Khan, N. Rajpoot, D. Treanor, and D. Magee, "A nonlinear mapping approach to stain normalization in digital histopathology images using image-specific color deconvolution," *IEEE Trans. Biomed. Eng.* 61(6), 1729–1738 (2014).
6. P. Salehi, A. Chalechale, "Pix2Pix-based Stain-to-Stain Translation: A Solution for Robust Stain Normalization in Histopathology Images Analysis," arXiv, 2002.00647 (2020).

7. A. Anghel, M. Stanisavljevic, S. Andani, N. Papandreou, J. H. Rüschoff, P. Wild, M. Gabrani, and H. Pozidis, "A High-Performance System for Robust Stain Normalization of Whole-Slide Images in Histopathology," *Front. Med.* **6**, 193 (2019).
8. M. T. Shaban, C. Baur, N. Navab, and S. Albarqouni, "StainGAN: Stain Style Transfer for Digital Histological Images," in *2019 IEEE 16th International Symposium on Biomedical Imaging (ISBI 2019)* (2019), pp. 953–956.
9. E. Reinhard, M. Adhikhmin, B. Gooch, and P. Shirley, "Color transfer between images," *IEEE Comput. Graph. Appl.* **21**(5), 34–41 (2001).
10. A. C. Ruifrok and D. A. Johnston, "Quantification of histochemical staining by color deconvolution," *Anal. Quant. Cytol. Histol.* **23** (4), 291–299 (2001).
11. M. Macenko, M. Niethammer, J. S. Marron, D. Borland, J. T. Woosley, Xiaojun Guan, C. Schmitt, and N. E. Thomas, "A method for normalizing histology slides for quantitative analysis," in *2009 IEEE International Symposium on Biomedical Imaging: From Nano to Macro (2009)*, pp. 1107–1110.
12. A. Vahadane, T. Peng, A. Sethi, S. Albarqouni, L. Wang, M. Baust, K. Steiger, A. M. Schlitter, I. Esposito, and N. Navab, "Structure-Preserving Color Normalization and Sparse Stain Separation for Histological Images," *IEEE Trans. Med. Imaging.* **35**(8), 1962–1971 (2016).
13. G. W. Gill, "Papanicolaou Stain," in *Cytopreparation: Principles & Practice* (Springer New York, 2013), pp. 143–189.
14. Y. Zheng, Z. Jiang, H. Zhang, F. Xie, D. Hu, S. Sun, J. Shi, and C. Xue, "Stain standardization capsule for application-driven histopathological image normalization," *IEEE J. Biomed. Heal. Inform.* **1** (2020).
15. N. Zhou, D. Cai, X. Han, and J. Yao, "Enhanced Cycle-Consistent Generative Adversarial Network for Color Normalization of H&E Stained Images," in *Medical Image Computing and Computer Assisted Intervention -- MICCAI 2019*, D. Shen, T. Liu, T. M. Peters, L. H. Staib, C. Essert, S. Zhou, P.-T. Yap, and A. Khan, eds. (Springer International Publishing, 2019), pp. 694–702.
16. J. Y. Zhu, T. Park, P. Isola, and A. A. Efros, "Unpaired Image-to-Image Translation Using Cycle-Consistent Adversarial Networks," in *Proceedings of the IEEE international conference on computer vision (2017)*, pp. 2242–2251.
17. D. Tellez, G. Litjens, P. Bándi, W. Bulten, J.-M. Bokhorst, F. Ciompi, and J. van der Laak, "Quantifying the effects of data augmentation and stain color normalization in convolutional neural networks for computational pathology," *Med. Image Anal.* **58**, 101544 (2019).
18. C. Shaojin, X. Yuyang, G. Qinquan, C. Gang, Z. Heijun, T. Tong, "Neural stain-style transfer learning using gan for histopathological images," arXiv, 1710.08543 (2017).
19. G. Lei, Y. Xia, D.-H. Zhai, W. Zhang, D. Chen, and D. Wang, "StainCNNs: An efficient stain feature learning method," *Neurocomputing* **406**, 267–273 (2020).
20. J. Yang, C. Liu, and L. Zhang, "Color space normalization: Enhancing the discriminating power of color spaces for face recognition," *Pattern Recognit.* **43**(4), 1454–1466 (2010).
21. Z. Wang, A. C. Bovik, H. R. Sheikh, and E. P. Simoncelli, "Image quality assessment: from error visibility to structural similarity," *IEEE Trans. Image Process.* **13**(4), 600–612 (2004).
22. A. Gupta, R. Duggal, S. Gehlot, R. Gupta, A. Mangal, L. Kumar, N. Thakkar, and D. Satpathy, "GCTI-SN: Geometry-inspired chemical and tissue invariant stain normalization of microscopic medical images," *Med. Image Anal.* **65**, 101788 (2020).
23. D. Tellez, M. Balkenhol, I. Otte-Höller, R. Van De Loo, R. Vogels, P. Bult, C. Wauters, W. Vreuls, S. Mol, N. Karssemeijer, G. Litjens, J. Van Der Laak, and F. Ciompi, "Whole-Slide Mitosis Detection in H&E Breast Histology Using PHH3 as a Reference to Train Distilled Stain-Invariant Convolutional Networks," *IEEE Trans. Med. Imaging* **37**(9), 2126–2136 (2018).
24. K. He, X. Zhang, S. Ren, and J. Sun, "Deep Residual Learning for Image Recognition," in *2016 IEEE Conference on Computer Vision and Pattern Recognition (2016)*, pp. 770–778.
25. J. Deng, W. Dong, R. Socher, L. Li, Kai Li, and Li Fei-Fei, "ImageNet: A large-scale hierarchical image database," in *2009 IEEE Conference on Computer Vision and Pattern Recognition (2009)*, pp. 248–255.